the effects of interaction of dipole and quadrupole oscillations, this may be due to the fact that Er^{166} is statically non-axial. Approximation of σ_γ by three (lorentzian) resonances of equal dipole strength yields for Er^{166} a non-axiality parameter $\gamma = 20 \pm 3°$.

Nucleus	σ_{int}, MeV-b	β	Q_0, b
Er^{166}	3.05 ± 0.3	0.33	7.76
Hf^{178}	3.16 ± 0.3	0.26	6.72

The table lists the values of the integral cross sections σ_{int} calculated from σ_γ and the deformation parameters β, as well as the values Q_0 of the intrinsic quadrupole moments of the nuclei, corresponding to the obtained values of β.

[1] B. I. Goryachev, B. S. Ishkhanov, V. G. Shevchenko, and B. A. Your'ev, Yad. Fiz. 7, 1168 (1968) [Sov. J. Nuc. Phys. 7, 698 (1968)].
[2] V. N. Orlin, Izv. AN SSSR ser. fiz. 37, 1107 (1973).
[3] B. I. Goryachev, Atom. Energ. 12, 245 (1962).
[4] N. N. Balamatov, B. I. Goryachev, and V. N. Orlin, Prib. Tekh. Eksp. No. 5, 245 (1971).
[5] B. I. Goryachev, Yu. V. Kuznetsov, and V. N. Orlin, ibid. No. 3, 64 (1972).
[6] A. N. Tikhonov, Dokl. Akad. Nauk SSSR 151, 501 (1963).
[7] B. S. Cook, Nucl. Instr. and Meth. 24, 256 (1963).
[8] H. Arenhövel, M. Danos, and W. Greiner, Phys. Rev. 157, 1109 (1967).
[9] S. F. Semenko, Yad. Fiz. 1, 414 (1965) [Sov. J. Nuc. Phys. 1, 295 (1965)].
[10] V. Rezwani, G. Gneuss, H. Arenhövel, Nucl. Phys. A180, 254 (1972).

RADIATIVE DECAY OF Σ^+ HYPERON

Yu. P. Malakyan
Physics Research Institute, Armenian Academy of Sciences

Submitted 11 November 1973
ZhETF Pis. Red. 19, No. 1, 68 – 72 (5 January 1974)

A low-energy theorem connecting the weak processes $\Sigma^+ \to p\gamma$ and $\Sigma^+ \to p\pi^0\gamma$ is derived by using the PCAC hypotehsis in standard fashion. Using this theorem, the amplitudes of the first transition are expressed in terms of the S-wave of the nonleptonic decay $\Sigma^+ \to p\pi^0$. The probability and asymmetry parameter of the $\Sigma^+ \to p\gamma$ decay are obtained. The results agree well with the experimental data. The difference between the presented analysis and the analogous approach in [2] is also explained.

In the present aritcle, using the PCAC hypothesis in the standard manner (see, e.g., [1]), we establish a low-energy theorem that connects the two decays $\Sigma^+ \to p\gamma$ and $\Sigma^+ \to p\pi^0\gamma$. This theorem allows us to express the amplitudes of the $\Sigma^+ \to p\gamma$ transition in terms of the amplitude of the S-wave of the $\Sigma^+ \to p\pi^0$ decay. The first approach of this type to radiative hyperon decay was used in [2]. However, the theoretical probability value obtained there for the only decay measured to date, $\Sigma^+ \to p\gamma$, turned out to be half the presently known experimental value. This discrepancy is due to the fact that the diagrams shown in Fig. 3 were not considered in [2][1]. Allowance for these diagrams leads to results that agree well with experiment.

The Lorentz and gauge invariance of the amplitude of the $\Sigma^+ \to p\gamma$ decay lead to the general expression

$$M_{\Sigma^+ \to p\gamma} = \langle p\gamma | H_w | \Sigma^+ \rangle = e\bar{U}_p (a + b\gamma_5) \gamma_\mu \gamma_\nu k_\mu \epsilon_\nu U_\Sigma . \quad (1)$$

We represent the parity-conserving part a of the transition in the form of a sum of a pole term which turns out to be determined by the diagram of Fig. 2 (see formulas (7a) and (6), and a contact part $\tilde{a}$:

$$a = a_{pol} + \tilde{a}.$$

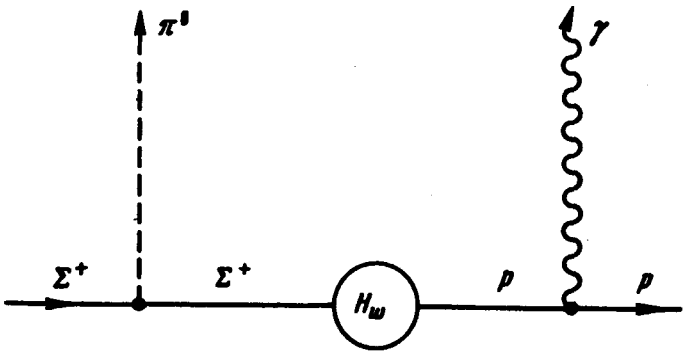

Fig. 1

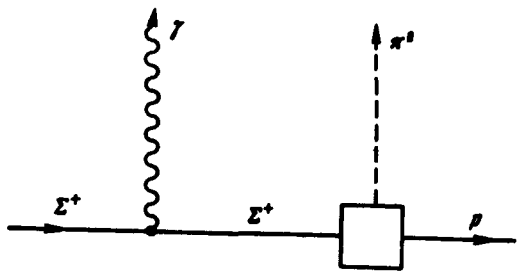

Fig. 2

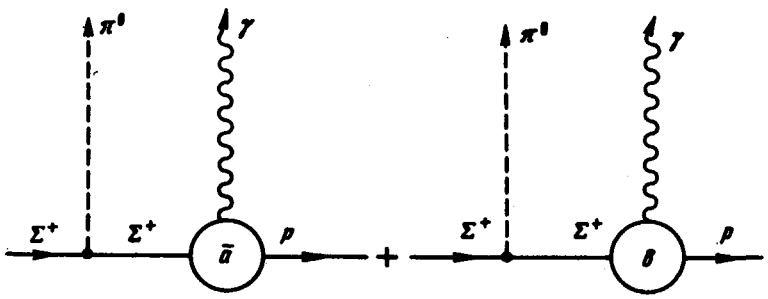

Fig. 3

The decay probability is expressed in terms of a and b as follows:

$$\Gamma(\Sigma^+ \to p\gamma) = \frac{a}{2}\left(\frac{m_\Sigma^2 - m_N^2}{m_\Sigma}\right)^3 (|a|^2 + |b|^2) \ .$$

We now consider the process

$$\Sigma^+ = p + \pi^0(q) + \gamma(k) \ . \tag{2}$$

Using in the reduction formula

$$M_2 = -i \int dx\, e^{iqx} (\Box - m_\pi^2) < p\gamma |\, T H_w(0)\, \phi^{(3)}(x) |\, \Sigma^+ >$$

the PCAC relation

$$\partial_\mu a_\mu^{(3)}(x) = m_\pi^2 F_\pi \phi^{(3)}(x) \ ,$$

and also the V - A symmetry property of the nonleptonic weak Hamiltonian H_W (no other assumptions are made concerning H_W)

$$[V^{(3)} - A^{(3)}, H_w] = 0, \quad A^{(3)} = \int d^3x\, a_0^{(3)}(\mathbf{x}, x_0) \tag{3}$$

we obtain in the limit as $q \to 0$ the equation

$$\lim_{q\to 0} M_2(q) = \frac{i}{2F_\pi} \langle p\gamma | H_w | \Sigma^+ \rangle + \lim_{q\to 0} q_\mu P_\mu(q), \tag{4}$$

where F_π is determined by the Goldberger-Treiman relation

$$F_\pi = \frac{m_N g_A / g_V}{g_{\pi N}}, \qquad g_A/g_V = 1{,}18, \quad g_{\pi N}^2/4\pi = 14{,}6,$$

and P_μ contains only Born terms, where the axial current is inserted in the middle of the external baryon lines. Similar diagrams are found also in $M_2(q)$, where, however, a π-meson line is attached to the external baryon lines instead of the current $a_\mu(x)$. To simplify the calculations we introduce a fictitious mass difference between the baryons in the matrix elements $\langle B|a_\mu|B\rangle$ and $\langle B|J_\pi|B\rangle$ and let this difference go to zero after taking the limit as $q \to 0$. Then the term $q_\mu P_\mu$ vanishes, and the entire pole term, which no longer has any singularities at $q = 0$, is obtained only from $M_2(q)$. It is easy to verify that the results are the same whether this procedure is used or whether the pole terms are calculated by using both terms $q_\mu P_\mu$ and $M_2(q)$.

We examine now the diagrams that will not be taken into account in the left-hand side of (4). These are, first, the diagrams of Fig. 1, the number of which, taking the permutation of the vertices γ_5, $\langle H_w \rangle$, and $\sigma_{\mu\nu}k_\nu$ into account, is six. These diagrams are calculated in the SU(3)-symmetry limit, i.e., writing the vertex $BB'\pi$ in the form

$$\langle B' | J_\pi^{(3)} | B \rangle = g_{B'B}^{(3)} \bar{U}_{B'} i\gamma_5 U_B$$

we use for $g^i_{B'B}$ the expression

$$i g^i_{B'B} = 2 g_{\pi N} [\epsilon f^i_{B'B} + i(1-\epsilon) d^i_{B'B}],$$

where f^i_{jk} and d^i_{jk} are the SU(3) structure constants. The electromagnetic vertex is taken in the form

$$\langle B | J_\mu^{e.m.} | B \rangle = -ie \bar{U}_B \sigma_{\mu\nu} k_\nu \frac{\mu_B}{2m_B} U_B$$

μ_B is the anomalous magnetic moment of the baryon. The charge vertex $e\bar{U}_B\gamma_\mu U_B$ will not be taken into account anywhere, since the calculations show that its contribution to the sum of the diagram vanishes in the limit as $q \to 0$.

The next class of diagrams is shown in Fig. 2, where the square denotes the S-wave part of the $\Sigma^+ \to p\pi^0$ decay. Further, if we express the amplitude of this transition on the mass shell in the form

$$M(\Sigma^+ \to p\pi^0) = \bar{U}_p (S_{\Sigma^+}(q^2) + \gamma_5 P_{\Sigma^+}(q^2)) U_\Sigma,$$

then we are left at $q \to 0$ only with the S-wave, and the pole diagrams in the P-wave are cancelled by some contact diagram that does not vanish at $q = 0$; the value of this diagram is determined in this limit just from the relation (we again introduce the fictitious mass difference)

$$\lim_{q\to 0} P^{\text{cont}}_{\Sigma^+} = -\lim_{q\to 0} P^{\text{pol}}_{\Sigma^+} = \left(\frac{g_{\pi N}}{2m_N} + \frac{g_{\pi\Sigma}}{2m_\Sigma}\right) T_{\Sigma^+ p}\, \bar{U}_p i\gamma_5 U_\Sigma, \tag{5}$$

where (see, e.g., [1])

$$T_{\Sigma^+ p} = \langle p | H_w | \Sigma^+ \rangle = -2iF_\pi S_{\Sigma^+}(0), \quad g_{\pi\Sigma} = 2\epsilon g_{\pi N}. \tag{6}$$

Consequently, one should consider the diagrams that take the contribution (5) into account. They are similar to those of Fig. 2, but the S-wave is replaced by the vertex (5). We denote the sum of these diagrams and of the diagrams of Fig. 1 by $ie\bar{U}_p B\gamma_5 \hat{k}\hat{\epsilon} U_\Sigma$, where

$$B = \frac{g_{\pi N} T_{\Sigma^+ p}}{2(m_\Sigma - m_N)}\left(\frac{\mu_p}{m_N^2} - 2\epsilon\frac{\mu_{\Sigma^+}}{m_\Sigma^2}\right).$$

Finally, the last group of diagrams (Fig. 3) takes into account the contribution of the transition $\Sigma^+ \to p\gamma$ to the process (2), and only the regular part a need be taken into account in the amplitude $\tilde{a}$. The sum of the diagrams of Fig. 3 is given by

$$\Sigma(\text{Fig.3}) = -ie\bar{U}_p(\tilde{a}\gamma_5 + b)\hat{k}\hat{\epsilon}U_\Sigma\left(\frac{1}{m_N} + 2\epsilon\frac{1}{m_\Sigma}\right)g_{\pi N}/2 .$$

We do not consider the diagrams that account for the contribution of the resonances and multiparticle intermediate states, assuming that their contributions are small. This is confirmed by the fact that the theoretical results obtained under this assumption coincide with the experimental data.

Comparing the coefficients preceding the structures $\bar{U}_p\gamma_5\hat{k}\hat{\epsilon}U_\Sigma$ and $\bar{U}_p\hat{k}\hat{\epsilon}U_\Sigma$ in the left and right sides of (4), we obtain

$$a_{\text{pol}} = \frac{T_{\Sigma^+ p}}{m_\Sigma - m_N}\left(\frac{\mu_{\Sigma^+}}{2m_\Sigma} - \frac{\mu_p}{2m_N}\right), \tag{7a}$$

$$\left.\begin{aligned} &\tilde{a} = -\chi b, \quad \chi = F_\pi g_{\pi N}\left(\frac{1}{m_N} + 2\epsilon\frac{1}{m_\Sigma}\right) \\ &b = (1-\chi^2)^{-1} 2F_\pi B \end{aligned}\right\} \tag{7b}$$

We present below the values for the decay probability and the asymmetry parameter

$$a = 2\text{Re}\, a^* b / |a|^2 + |b|^2$$

We chose for the total magnetic moment of Σ^+ the experimental value 2.57 (in units of $eh/2m_Nc$). The value of $T_{\Sigma^+ p}$ is determined from (6), and that of S_{Σ^+} from the experimental probability of the $\Sigma^+ \to p\pi^0$ decay (see [3] concerning all the experimental data). The value of ϵ was taken to be 0.37 [4].

	$\lvert\tilde{a}\rvert \cdot 10^{10}$ MeV^{-1}	$\lvert a_{\text{pol}}\rvert \cdot 10^{10}$ MeV^{-1}	$\lvert b\rvert \cdot 10^{10}$ MeV^{-1}	$\Gamma_{\Sigma^+ \to p\gamma} \cdot 10^{14}$ MeV	a
Theory	1,59	0,01	0,83	1,026	- 0,81
Expt.	-	-	-	$1,01 \pm 0,14$	$-1,02^{+0,52}_{-0,42}$

It is seen from the table that the prediction of the PCAC hypothesis is in good agreement with experiment. We call attention to the fact that the contact part $\tilde{a}$, which is not taken into account in [3], makes the main contribution to the probability. It is seen from (7) that all the amplitudes of the $\Sigma^+ \to p\gamma$ decay are expressed in terms of one single quantity $\langle p|H_W|\Sigma^+\rangle$, for which the $\Delta T = 1/2$ rule is satisfied; this rule should therefore hold also for the radiative decay of hyperons.

Similar reasoning can be applied also to the decays $A \to n\gamma \equiv -(\Lambda, \Sigma)\gamma$. The results for them will be published separately.

The author is deeply grateful to B. L. Ioffe for a discussion and valuable remarks.

[1] Each figure shows only one of a given class of diagrams; the others are obtained by permutation of all the vertices contained in the given diagram.

[1] A. I. Vainshtein and V. I. Zakharov, Usp. Fiz. Nauk 100, 225 (1970) [Sov. Phys.-Usp. 13, 73 (1970)].
[2] M. A. Ahmed, Nuovo Cim. 58A, 728 (1968).
[3] Rev. of Part. Properties, Rev. Mod. Phys. 45, No. 2, part II, 1973.

[4] L.-M. Chounet, G.-M. Gillard, and M. K. Gaillard, Phys. Rep. 4, 201 (1972).

In the article by Yu. P. Malakyan, Vol. 19, No. 1, in the left-hand side of Eq. (4) (p. 46), no account was taken of the pole diagrams with contact vertex $\overline{B}B\pi\pi^0\gamma$, the contribution of which is completely cancelled by the contribution of the remaining pole diatrams, and the amplitudes $\tilde{a}$ and b are determined only by the contribution of the non-pole part of the amplitude $M_2(q)$. This contribution is not small, and the results presented in the article no longer hold.